

# Combustion Characteristics of Aluminum Hydride at Elevated Pressure and Temperature

T. Bazyn,\* R. Eyer,\* H. Krier,<sup>†</sup> and N. Glumac<sup>‡</sup>

*University of Illinois at Urbana—Champaign, Urbana, Illinois 61801*

**A comparison of the combustion characteristics of aluminum hydride and aluminum with respect to combustion time and temperature at elevated pressures in carbon dioxide and oxygen has been performed using a shock tube. For a wide range of oxidizer concentrations, the combustion time of 5–10  $\mu$  aluminum hydride is very similar to that of aluminum. Gas-phase temperatures measured by aluminum monoxide (AlO) emission and absorption spectroscopy, as well as solid product temperatures measured by two-color pyrometry, yield very similar values for both materials (to within experimental uncertainty). Observations of hydroxyl (OH) emission behind the incident shock suggest that hydrogen desorbs at temperatures well below the ignition threshold for aluminum. These observations are all consistent with the oxidation of aluminum hydride involving a rapid dehydrogenation step, followed by combustion of the remaining aluminum.**

## Introduction

**A**LUMINUM hydride ( $\text{AlH}_3$ ) has been proposed as an additive to solid rocket propellants and high explosives to increase the performance of these materials. Similar to other metal hydrides, aluminum hydride, or alane, has a high energy density and offers significant advantages over currently used solid-rocket-motor (SRM) propellant metal additives. Aluminum hydride contains approximately 10% wt. hydrogen and has a higher density of hydrogen (0.148 g  $\text{H}_2/\text{cm}^3 \text{AlH}_3$ ) than liquid hydrogen. The high hydrogen density and the high degree of energy release from the combustion of both aluminum and hydrogen make alane an ideal additive for solid propellants or explosives.

U.S. Department of Defense predictions indicate that replacing aluminum with alane will result in at least a 10% gain in specific impulse over currently used SRM propellants, and that it can provide up to a 20% gain when used in combination with ammonium dinitramide.<sup>§</sup> Because of the low density of aluminum hydride, it would be most advantageous in upper-stage motors and space motors where reduced density is advantageous. The increase in specific impulse translates into a 23% increase in payload for the Titan IV launch vehicle and a 30% increase in range for a typical strategic missile.<sup>§</sup> The reduction in size at a similar performance for these applications is equally impressive. In volume limited applications, aluminum hydride does not provide a significant performance gain because of its low density, but it does provide a reduction in weight. Other practical applications of aluminum hydride are as a chemical reducing agent or a hydrogen storage device for fuel cells.

Nonsolvated aluminum hydride exists in six crystalline phases, each with different physical properties.  $\alpha$ -alane is the most stable phase, forming crystals with hexagonal or cubic shapes. Details on the synthesis and structure of the other alane phases are provided in Ref. 1. The  $\alpha$  phase can be made more stable using technology developed in the former Soviet Union and described in U.S. Patent 6228338 B1 (Ref. 2). The research presented here focuses solely on

this stabilized  $\alpha$  phase, as it is the most stable form and is the only form with a long-enough shelf life to be considered as an additive to propellants.

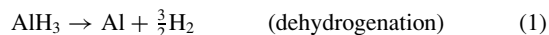
The thermodynamic properties of aluminum hydride were experimentally confirmed by Sinke et al.<sup>3</sup> The heat of formation was found to be approximately  $-2.7$  kcal/mole.

Combustion data on aluminum hydride are scarce. Selezenev et al.<sup>4</sup> compared the effects of aluminum and aluminum hydride on the detonation and performance of composite explosives using models and some experimental results. The adiabatic expansion work of the explosive was increased significantly with the addition of aluminum hydride to ammonium nitrate, pentaerythritoltetranitrate (PETN), and cyclotrimethylenetrinitramine (RDX). Also, the detonation velocity is higher for the addition of  $\text{AlH}_3$  to the preceding fuels than for the addition of aluminum. The study also shows that there is an increase in detonation velocity when aluminum and aluminum hydride are added to ammonium nitrate, whereas there is a decrease in detonation velocity when these materials are added to PETN and RDX. However,  $\text{AlH}_3$  still provides better performance than aluminum in these cases.

Il'in et al.<sup>5</sup> performed experimental research on the combustion of aluminum hydride in air at 1 atm. Aluminum hydride was found to burn in a method very similar to that of elemental aluminum, except for an additional stage of hydrogen combustion at relatively low temperatures.

Because there are few studies involving the combustion of aluminum hydride, there exists the need to establish the burning characteristics of alane in order to consider it for applications where it would replace aluminum. If the burning characteristics of the two materials are similar, then the replacement of aluminum with alane in energetic materials applications would be significantly facilitated.

Of particular interest is the timescale for the release of hydrogen by alane. Previous work has suggested that aluminum hydride will rapidly dehydrogenate at low temperatures, leaving the aluminum metal behind. Thus, we anticipate that in general combustion environments aluminum hydride will react via a two-step mechanism:



If the dehydrogenation step is slow, then there is the possibility of inhibiting the rather fast kinetics of aluminum particle combustion. On the other hand, early in the combustion process there can be significant amounts of hydrogen near the particle surface, which will increase the conductivity and diffusivity of the gas phase. Because transport properties play a strong role in diffusion-limited particle burning, the near-surface hydrogen could potentially accelerate particle ignition and combustion.

Received 16 June 2003; revision received 30 October 2003; accepted for publication 4 November 2003. Copyright © 2003 by the American Institute of Aeronautics and Astronautics, Inc. All rights reserved. Copies of this paper may be made for personal or internal use, on condition that the copier pay the \$10.00 per-copy fee to the Copyright Clearance Center, Inc., 222 Rosewood Drive, Danvers, MA 01923; include the code 0748-4658/04 \$10.00 in correspondence with the CCC.

\*Graduate Student, Mechanical and Industrial Engineering Department, College of Engineering, 1206 West Green Street.

<sup>†</sup>Professor, Mechanical and Industrial Engineering, Fellow AIAA.

<sup>‡</sup>Associate Professor, Mechanical and Industrial Engineering, Member AIAA.

<sup>§</sup>Data available online at <http://www.dtic.mil/dust/cgr/navy00cgr.html#navy3>.

## Specific Objectives

The research presented here attempts to address the combustion of aluminum hydride compared to aluminum at conditions similar to that found in a SRM. The oxidizing atmospheres are varied, using various fractions of oxygen and carbon dioxide in an inert gas. Burn times and burn temperatures are compared for Al and  $\text{AlH}_3$  particles of the same size distribution. Because these are some of the most critical parameters in the performance of additive materials to SRM propellants, any significant differences between the values obtained for Al and  $\text{AlH}_3$  would be expected to impact the performance of an SRM in a measurable fashion.

## Experimental

The experiments were conducted in our shock-tube facility, which has been described in detail in previous publications<sup>6</sup> and is shown schematically in Fig. 1. In brief, an 8.38-m shock tube is used to generate a high temperature (here 2650 K) and elevated pressure (8.5 atm) environment behind the shock reflected off the tube end wall. A small sample ( $\sim 1$  mg) of powder is injected into the tube just after the tube is filled with gases of the requisite composition and prior to the diaphragm bursting. The injector produces a dilute cloud of the particulates, which is heated by the incident and reflected shocks. The particles burn in the tube under highly controlled temperature, pressure, and composition conditions. Emission from the burning cloud is observed through four sapphire windows by photodiodes with interference filters to isolate specific spectral features, by spectrometers, and by a two-color pyrometer. For some measurements, the powder is placed on a knife edge near the end wall and dispersed by the incident shock, producing a more localized burning cloud.

Photometry of the combustion event is accomplished by looking at the AIO emission near 486 nm through an interference filter that captures the bulk of the  $\Delta v = 0$  band of the  $B^2\Sigma^+ \rightarrow X^2\Sigma^+$  band of AIO. The burn time for a particular combustion event is calculated by determining the full width at half-maximum (FWHM) of the intensity vs time trace.

For the emission spectroscopy measurements we use an f/5 50-mm spectrometer with a 2:1 demagnification and a Starlight Express 516 charge-coupled device detector. This arrangement yields 2 Å resolution of the  $\Delta v = -1$  band, which has a structure that is very sensitive to temperature in the range of expected temperatures (2500–4500 K). Spectra are fit by a spectral model to a temperature and optical depth using established spectroscopic relations.<sup>7</sup>

Pyrometry measurements are made with a two-color pyrometer using photomultipliers and interference filters centered at 700 and 825 nm. Emission spectra were taken to verify that the signal at these wavelengths was blackbody emission from solids and not molecular emission.

All powders were sieved through a 10- $\mu$  sieve, but did not pass through a 5- $\mu$  sieve. The aluminum was purchased from Aldrich, Inc. An scanning electron microscope (SEM) photograph of the alane powder is shown in Fig. 2.

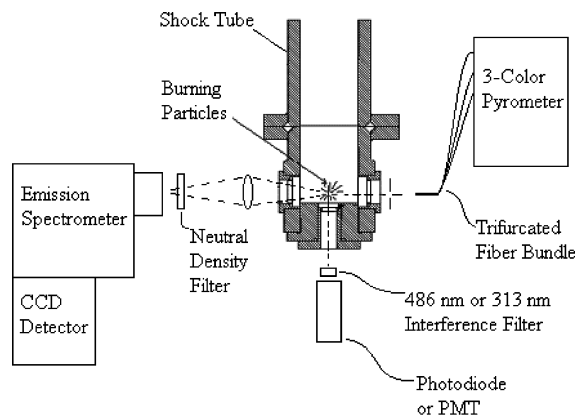


Fig. 1 Schematic of the diagnostic setup in the test section of the UIUC 8.4 m shock-tube facility.

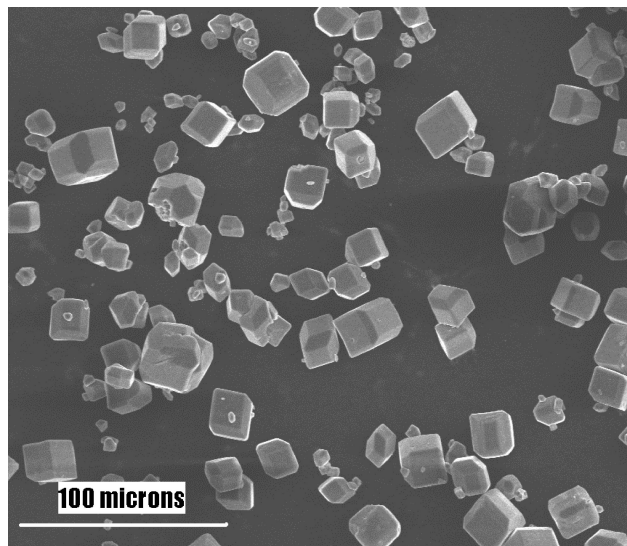


Fig. 2 SEM photograph of the aluminum hydride powder used in this study.

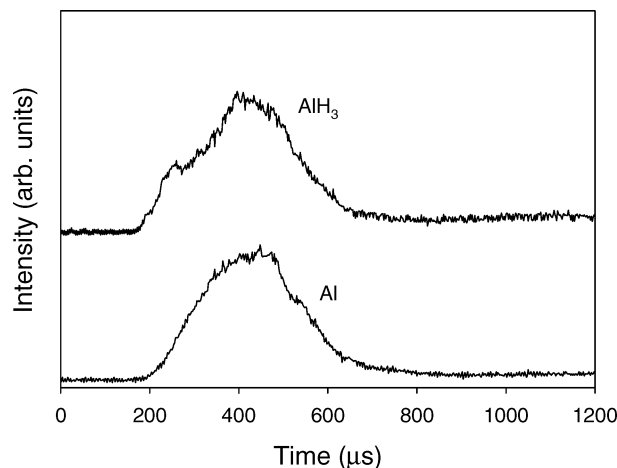


Fig. 3 Intensity at 486 nm for Al and  $\text{AlH}_3$  burning in 25%  $\text{CO}_2$  in Ar at 8.5 atm and 2650 K. A time of zero corresponds to the reflection of the incident shock off the end wall of the shock tube. The traces are the average over three tests.

## Results

Burn times were investigated for aluminum and aluminum hydride for two oxidizers,  $\text{O}_2$  and  $\text{CO}_2$ . In both cases, the oxidizer was diluted in argon, and the concentration of the oxidizer was varied in the 10–60% range. The conditions behind the reflected shock were held constant at  $2650 \text{ K} \pm 75 \text{ K}$  and  $8.5 \text{ atm} \pm 0.5 \text{ atm}$ . Tests were repeated at least twice at each condition. Figure 3 shows the average of three tests of the intensity vs time traces for aluminum and aluminum hydride for 25%  $\text{CO}_2$  in Ar, and Fig. 4 shows the same data for 60%  $\text{CO}_2$ . As can be seen from these plots, there is very little difference in the temporal profile of the light emission for the two species. Using any of the common methods to convert an intensity versus time trace to a burn time (i.e., FWHM, percent area, percent height<sup>8</sup>), the burn times are very similar for these two materials. In addition, the induction times are also very similar. From these data, it appears that the combustion of alane and aluminum follow very similar time scales.

Summary data for burn times in  $\text{CO}_2$  and  $\text{O}_2$  are shown in Figs. 5 and 6, respectively. Though there is some scatter in the data, especially for alane in  $\text{O}_2$ , the mean values of the burn times agree to within uncertainty for all of the cases investigated.

Optical emission spectroscopy results were likewise very similar for the two powder species. The AIO emission temperature that

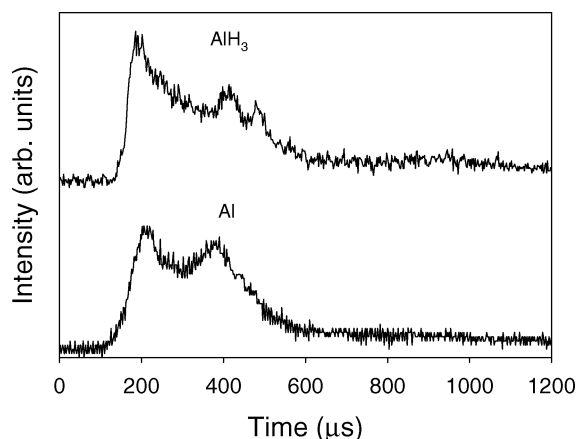


Fig. 4 Intensity at 486 nm for Al and  $\text{AlH}_3$  burning in 60%  $\text{CO}_2$  in Ar at 8.5 atm and 2650 K. The traces are the average over three tests.

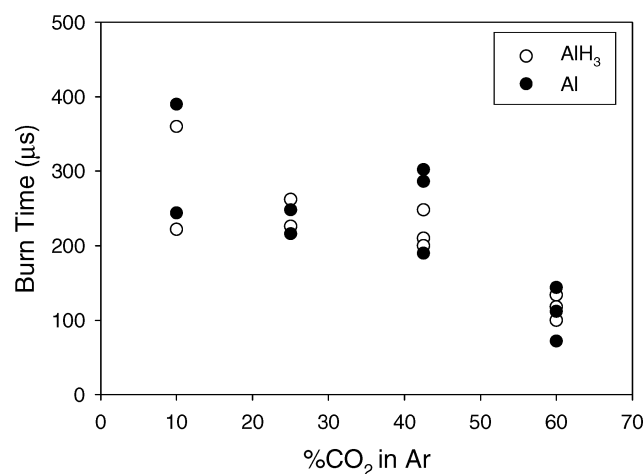


Fig. 5 FWHM burn times for Al and  $\text{AlH}_3$  at 8.5 atm and 2650 K for varying amounts of  $\text{CO}_2$  in Ar. Each point represents a single test.

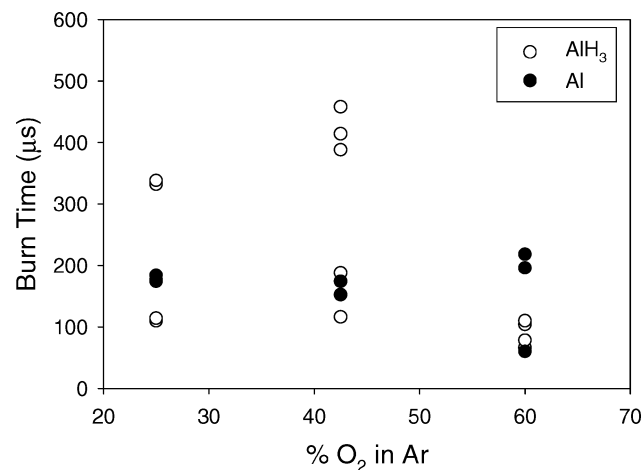


Fig. 6 FWHM burn times for Al and  $\text{AlH}_3$  at 8.5 atm and 2650 K for varying amounts of  $\text{O}_2$  in Ar. Each point represents a single run.

is fit by the spectroscopic model was found to vary with optical depth, which is dependent on the local powder loading in the focal volume probed by the spectrometer. This depth varies from run to run. The optical depth for a given run is determined in the spectrum fitting procedure. For cases approaching optically thin conditions, the observed temperatures were 3000–3300 K. Both aluminum and aluminum hydride show roughly the same dependence of AIO emission temperature on optical depth, as well as the same temperatures, for combustion in both  $\text{CO}_2$  (Fig. 7) and  $\text{O}_2$  (Fig. 8). Though the

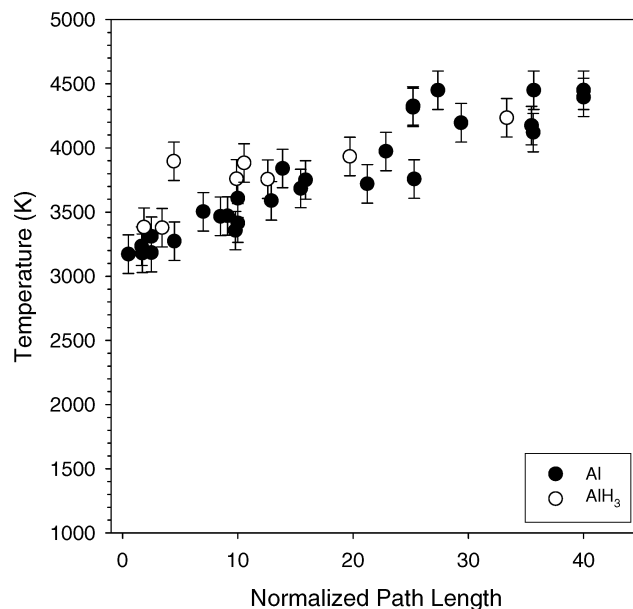


Fig. 7 Optical emission temperature from AIO as a function of AIO optical depth for the combustion of Al (●) and  $\text{AlH}_3$  (○) in carbon dioxide and argon at 2650 K and 8.5 atm.

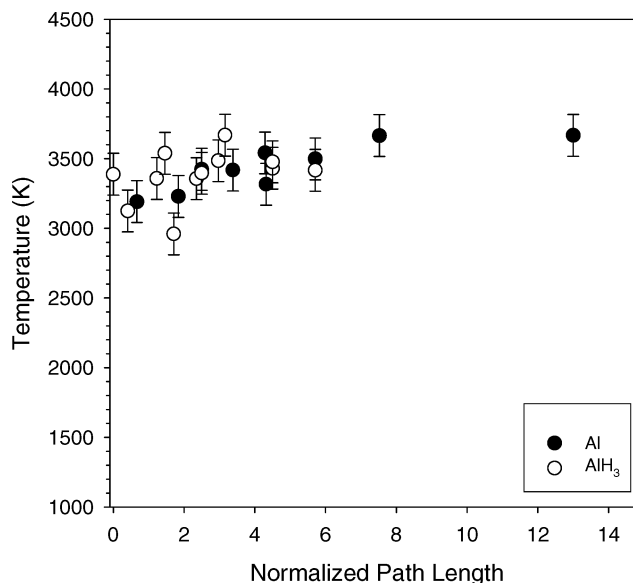


Fig. 8 Optical emission temperature from AIO as a function of AIO optical depth for the combustion of Al (●) and  $\text{AlH}_3$  (○) in oxygen and argon at 2650 K and 8.5 atm.

interpretation of this single temperature value is somewhat uncertain because of the optical depth effects and the uncertain nature of the spatial temperature distribution around a burning particle, it is clearly a strong function of the gas temperature surrounding the burning particle, and thus if both particles show similar values then similar temperatures and temperature distributions are expected. We have also taken a small series of absorption spectra for Al and  $\text{AlH}_3$  and compared the fit temperatures to those obtained in emission. These measurements yield very similar temperatures.

The pyrometry measurements show similar results to the spectroscopic measurements, as shown in Fig. 9. Using the emission at 700 and 825 nm, the two-color temperatures over the bulk of the combustion event are roughly the same, and in the range of 2500–3000 K, which is slightly lower than the calculated adiabatic flame temperature (AFT) of Al in  $\text{CO}_2$  at 3090 K, based on room temperature reactants,<sup>9</sup> and significantly lower than the AFT of 4030 K based on reactants at 2650 K.

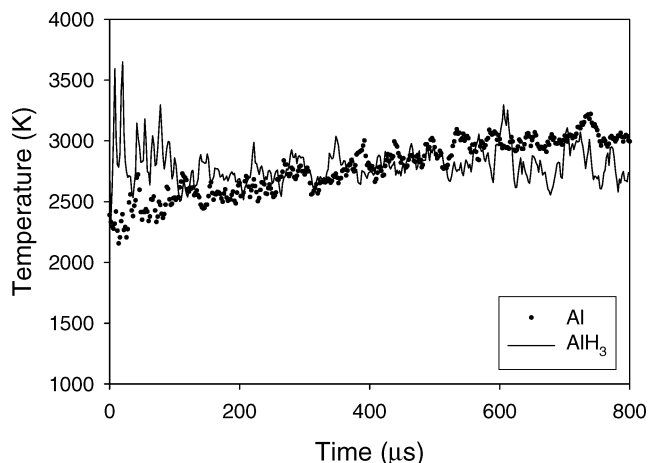


Fig. 9 Two-color pyrometry data for Al and  $\text{AlH}_3$  burning in 30%  $\text{CO}_2$  at 8.5 atm and 2650 K.

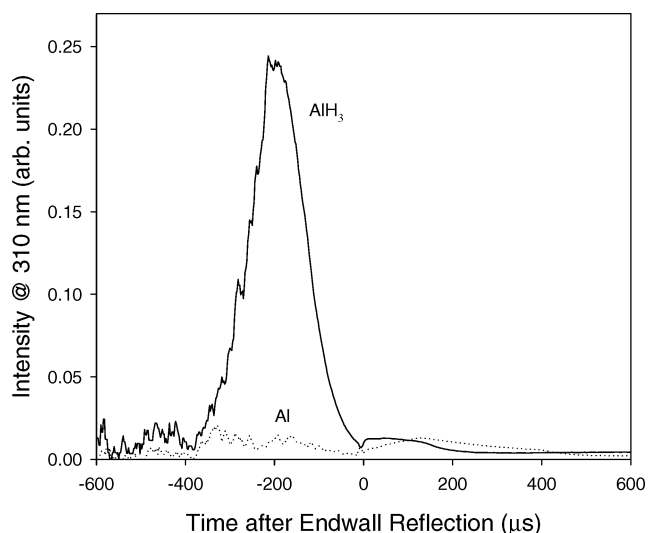


Fig. 10 OH emission signal, scaled by multiplication by the distance from detector to the incident shock, vs time for aluminum and aluminum hydride powders in 30%  $\text{O}_2$  in Ar. Conditions behind the incident shock were 0.91 atm and 1470 K.

Conditions behind the incident shock are approximately 1 atm and 1000–1500 K. The injected powders experience these conditions for approximately 400  $\mu\text{s}$  before the shock reflects off the end wall and heats the powders to 2650 K. The conditions behind the incident shock are not hot enough to ignite the aluminum, but might be hot enough to dehydrogenate the alane. If this is the case, then dehydrogenation will leave the 5–10- $\mu$ , primarily aluminum particles in front of the reflected shock. It would then be likely that ignition and combustion behavior of these particles would be similar to identically sized pure aluminum particles. To investigate this possibility, we mounted a 313-nm interference filter at the end-wall window in front of a photomultiplier. Kinetics calculations indicate that any hydrogen produced (atomic or molecular) behind the incident shock would react very quickly with the oxygen at 1 atm and 1000–1500 K, and thus we might expect to see some thermal or chemiluminescent OH emission around 313 nm. The results of this experiment are shown in Fig. 10. We have scaled the emission signal by multiplying by the distance between detector and shock front squared to account for the change in collection efficiency as the shock approaches the detector. There is a significant emission at 313 nm in the case of  $\text{AlH}_3$ , and this emission appears very soon after the incident shock passes the particle cloud. The intensity of the emission peaks then decreases before the incident shock hits the end wall, suggesting that the dehydrogenation is mostly complete

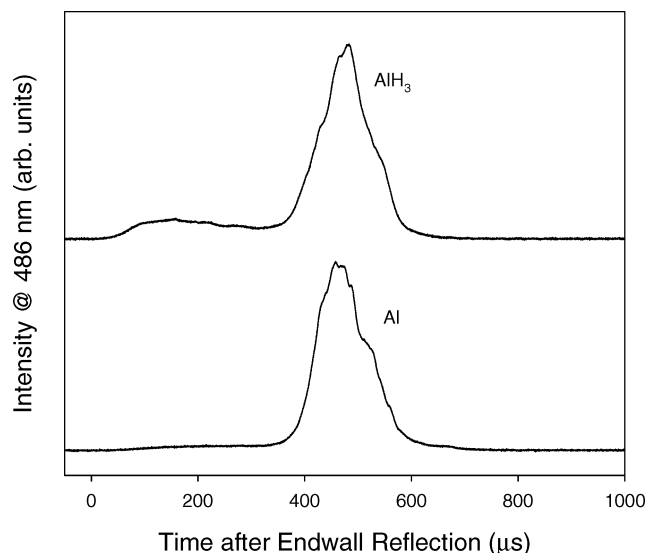


Fig. 11 AIO emission intensity at 486 nm vs time for aluminum and aluminum hydride particles loaded on a knife blade within 1 cm of the end wall and burning in 60%  $\text{CO}_2$  in Ar. The conditions behind the reflected shock were 8.5 atm and 2650 K.

in the 400  $\mu\text{s}$  that the particles are exposed to the gases behind the incident shock. For the aluminum case, there is no emission seen under the identical conditions.

Conditions in which particles are exposed quickly to temperatures high enough to ignite aluminum (as opposed to the two stage heating—behind incident then reflected shocks) can be achieved by loading particles very near the end wall. Under these conditions, particles are exposed to the incident shock for only a few microseconds before the arrival of the reflected shock. If the dehydrogenation step were inhibiting combustion, then we would expect to see a slower burn time under these conditions for  $\text{AlH}_3$  than aluminum. However, as seen in Fig. 11, this is not the case. Both powders burn similarly under these conditions as well.

## Discussion and Analysis

For cases in which the particles experience an extended period of time in the gases behind the incident shock, essentially all combustion parameters—burn time, ignition time, temperature of the solid and gas phase during burning—are nearly identical. The OH emission results suggest that dehydrogenation is mostly complete before the incident shock reaches the end wall, and thus the particles that burn behind the reflected shock are primarily aluminum. If the dehydrogenated particles remain at the same size as the initial alane particles, it is not entirely unexpected that burning characteristics of the resultant powders would be similar to identically sized aluminum under diffusion limited conditions, even though they contain less mass of aluminum. Perhaps the most important additional result from these experiments is that the dehydrogenation is rapid (on the scale of 100  $\mu\text{s}$ ) at the fairly low temperatures behind the incident shock. Further experiments to quantify dehydrogenation kinetics are currently underway.

Based on the results of end-wall loading, it can be further surmised that the dehydrogenation step is sufficiently faster than ignition and combustion of 5–10- $\mu$  particles. Furthermore, the presence of hydrogen around the particle in the early stages of combustion does not appear to either inhibit or enhance the combustion rate in a significant fashion. It might be logical then to speculate that the simple replacement of aluminum with aluminum hydride in SRM applications would not result in significant changes in the metal burning timescales, but would offer the enhanced energy release of the more energetic  $\text{AlH}_3$ .

The typical gas velocities at the surface of a burning propellant in an SRM are of the order of 1–10 m/s. If the timescale for hydrogen release at elevated pressures is the same as observed in our experiments, then a dehydrogenation time of a few hundred microseconds

would imply that hydrogen is released within the first millimeter above the burning propellant and thus will react in the propellant combustion zone(s) with the gaseous species evolved from the propellant surface. These gases would then be slightly more fuel rich, and it is likely that some optimization of the propellant composition to take advantage of this hydrogen would yield further increases in performance. The remaining aluminum would then burn further downstream as it does in current aluminized propellant formulations. Experiments in actual solid rockets would be useful in verifying any changes in flame structure caused by the replacement of aluminum with alane.

The pressures investigated in this study are still low compared to typical SRM conditions. In extrapolating our results to pressures in the 50–100 atm range, one effect of concern might be any change in the dehydrogenation temperature of alane. LeChatelier's principle suggests that elevated pressures would inhibit the release of hydrogen, leading to a higher dehydrogenation temperature, though this would likely be a weak effect. Further study is required to assess whether this change is large enough to delay dehydrogenation in an SRM until the particles have passed the primary flame zone.

Other general issues with aluminum hydride that deserve further consideration are whether alane ignites earlier than aluminum (because it presumably does not have the same  $\text{Al}_2\text{O}_3$  oxide coating as pure Al), whether alane has superior agglomeration resistance than aluminum, and whether alane is stable in real propellant mixtures under actual operating conditions including high vibrational loading.

### Summary

Our results suggest that replacing aluminum with alane in a solid rocket motor will result in a release of hydrogen very near the burning propellant surface. This hydrogen will likely burn with the decomposition products of the oxidizer. The remaining aluminum will burn very similarly (i.e. at similar rates and temperatures) to the way in which pure aluminum currently burns in SRMs.

### Acknowledgments

This work has been supported by the Office of Naval Research under Contract N00014-01-1-0899. The project monitor is Judah

Goldwasser. The SEM photography was carried out in the Center for Microanalysis of Materials, University of Illinois, which is partially supported by the U.S. Department of Energy under Grant DEFG02-91-ER45439.

### References

- <sup>1</sup>Brower, F. M., Matzek, N. E., Reigler, P. F., Rinn, H. W., Roberts, C. B., Schmidt, D. L., Snover, J. A., and Terada, K., "Preparation and Properties of Aluminum Hydride," *Journal of the American Chemical Society*, Vol. 98, No. 9, 1976, pp. 2450–2453.
- <sup>2</sup>Petrie, M. A., Bottaro, J. C., Schmitt, R. J., Penwell, P. E., and Bomberger, D. C., "Preparation of Aluminum Hydride Polymorphs, Particularly Stabilized  $\alpha\text{-AlH}_3$ ," U.S. Patent No. US 6,228,338 B1, 8 May 2001.
- <sup>3</sup>Sinke, G. C., Walker, L. C., Oetting, F. L., and Stull, D. R., "Thermodynamic Properties of Aluminum Hydride," *Journal of Chemical Physics*, Vol. 47, No. 8, 1967, pp. 2759–2761.
- <sup>4</sup>Selezenov, A. A., Kreknnin, D. A., Lashkov, V. N., Lobanov, V. N., and Fedorov, A. V., "Comparative Analysis of the Effects of Aluminum and Aluminum Hydride on the Detonation Parameters and Performance of Mixed Explosives," *Proceedings of the 11th International Detonation Symposium*, edited by J. M. Short and J. E. Kennedy, Office of Naval Research, Arlington, VA, 1998, pp. 231–236.
- <sup>5</sup>Il'in, A. P., Bychin, N. V., and Gromov, A. A., "Products of Combustion of Aluminum Hydride in Air," *Combustion, Explosion, and Shock Waves*, Vol. 37, No. 4, 2001, pp. 490, 491.
- <sup>6</sup>Servaites, J., Krier, H., Melcher, J. C., and Burton, R. L., "Aluminum Particle Ignition and Combustion Using a High-Pressure Shock Tube," *Combustion and Flame*, Vol. 125, No. 1/2, 2000, pp. 1038–1054.
- <sup>7</sup>Arnold, J. O., Whiting, E. E., and Lyle, G. C., "Line by Line Calculation of Spectra from Diatomic Molecules and Atoms Assuming a Voigt Line Profile," *Journal of Quantitative Spectroscopy and Radiative Transfer*, Vol. 9, No. 6, 1969, pp. 775–798.
- <sup>8</sup>Olsen, S. E., and Beckstead, M. W., "Burn Time Measurements of Single Aluminum Particles in Steam and  $\text{CO}_2$  Mixtures," *Journal of Propulsion and Power*, Vol. 12, No. 4, 1996, pp. 662–671.
- <sup>9</sup>Rossi, S., Dreizen, E. L., and Law, C. K., "Combustion of Aluminum Particles in Carbon Dioxide," *Combustion Science and Technology*, Vol. 164, No. 1, 2001, pp. 209–237.